JOURNAL OF MATERIALS SCIENCE 25 (1990) 1863–1871

Anisotropy of radiation-induced degradation in mechanical properties of fabric-reinforced polymer–matrix composites

S. EGUSA
Takasaki Radiation Chemistry Research Establishment, Japan Atomic Energy Research Institute, Takasaki-shi, Gunma 370-12, Japan

Four kinds of fabric-reinforced polymer–matrix composites (filler: E-glass or carbon fabric; matrix: epoxy or polyimide resin) were irradiated with ^{60}Co γ-rays or 2 MeV electrons at room temperature. Three-point bend tests were then carried out at 77 K and at room temperature in a 45° direction from warp to fill. Comparison of the degradation behaviour among these composites reveals that the glass–epoxy and glass–polyimide composites are quite similar to each other in the dose dependence of the ultimate interlaminar shear strength at each test temperature. This result suggests that the radiation damage at the fibre–matrix interface decreases the contribution of the chemical bond mode to the total bond strength at the interface, thus decreasing the composite shear strength with increasing dose. For the carbon–epoxy and carbon–polyimide composites, on the other hand, the shear strength at room temperature changes little even after irradiation up to 140 MGy, while the shear strength at 77 K decreases monotonically with increasing dose. These findings suggest that the fibre–matrix bond strength due to the friction force mode is quite insensitive to radiation, thus resulting in the dose-independent shear strength at room temperature. At 77 K, however, the friction force mode fails to function properly because of the brittleness of the matrix resin, and consequently the composite shear strength decreases with increasing dose owing to a resulting increase in the matrix brittleness.

1. Introduction

In a previous paper [1], the author reported a work on the radiation-induced degradation in the mechanical properties of polymer matrix composites. The work has shown that the dose dependence of the composite ultimate strength depends not only on the combination of fibre and matrix in the composite but also on the temperature during the mechanical test. It was also shown that a relationship exists between the composite ultimate strain and the matrix ultimate strain, thus clarifying the degradation mechanism that the dose dependence of the composite strength is virtually determined by a change in the matrix ultimate strain due to irradiation. Based on this mechanism, the author constructed a composite failure model which possibly explains the dose dependence of the ultimate strength for any type of composite at any test temperature. The model was, in fact, valid at least for four kinds of polymer matrix composites studied in the previous work [1].

In that work the mechanical test was performed only in the warp direction of plain-woven fabrics. At present, therefore, it is unknown whether the above-mentioned degradation mechanism for the warp direction holds also for directions other than the warp and fill. The elucidation of this problem will be very useful for further the fundamental understanding of the degradation behaviour of polymer matrix composites to be used in fusion magnets [2, 3] or in space vehicles [4, 5].

In the present work, four kinds of fabric-reinforced polymer–matrix composites were cut into rectangular specimens having the length axis in a 45° orientation with respect to the warp and fill. The 45° specimens were irradiated at room temperature with γ-rays from a ^{60}Co source or with 2 MeV electrons from an accelerator. Three-point bend tests were then carried out at 77 K and at room temperature. Comparison of the degradation behaviour among these composites revealed that the glass–epoxy and glass–polyimide composites are quite similar to each other in the dose dependence of the ultimate interlaminar shear strength at each test temperature. Such a similarity was observed also in a comparison between the carbon–epoxy and carbon–polyimide composites. The glass and carbon fibre composites, however, were found to differ essentially from each other in the degradation behaviour. The present paper mainly describes the dose dependence of the composite mechanical properties in a 45° direction from warp to fill. On the basis of the dose dependence, a possible mechanism of the composite degradation for the 45° direction is discussed.

0022–2461/90 $03.00 + .12

2. Experimental details

The composite materials studied here were the same type as those used in the previous work [1]. The reinforcing filler was a plain-woven E-glass fabric (Kanebo KS-1210) treated with a silane coupling agent (γ-glycidoxypropyltrimethoxysilane) or a plain-woven carbon fabric (Torayca No. 6142) treated with an epoxy sizing agent. The matrix resin was an epoxy of tetraglycidyl diaminodiphenyl methane (TGDDM) cured with diamino diphenyl sulphone (DDS) or a polyimide of polyaminobis-maleimide (Kerimid 601). By a combination of these fillers and resins, four kinds of fabric-reinforced polymer-matrix composites were prepared. The thickness of these laminate plates was between 1.7 and 2.3 mm, and the volume fraction of fibres was between 57 and 63%. Further details are described elsewhere [1].

The laminate plates were cut into rectangular specimens of 6.4 mm width and 70 mm length or specimens of 12.0 mm width and 70 mm length. The cutting was made so that the 70 mm axis was in a 45° orientation with respect to the warp and fill, thus obtaining 45° specimens. For comparison, rectangular specimens having the 70 mm axis parallel to the warp direction were also cut from the same laminate plates, thus obtaining 0° specimens.

The irradiation procedures with ^{60}Co γ-rays and 2 MeV electrons are described elsewhere [1]. Both irradiations were carried out in air at room temperature with the absorbed dose rate of about 0.021 MGy h^{-1} for γ-rays and about 11.5 MGy h^{-1} for electrons. In the present work, the electron irradiation was carried out only for the glass–epoxy composite, while for the other composites the irradiation was made with γ-rays. In this connection, it is worth noting that the irradiation effects of electrons have been confirmed to be almost the same as those of γ-rays for 0° specimens of the glass–epoxy composite [1].

The mechanical test apparatus and procedures for three-point bend tests were essentially the same as those reported earlier [1]. All specimens were tested at 77 K and at room temperature at a crosshead speed of 0.6 mm min^{-1}, except that the tests of 45° specimens at room temperature were made at a crosshead speed of 1.2 mm min^{-1}. These tests were carried out at the span length of 20 mm unless otherwise noted in the text. The load was applied in the direction normal to the laminate planes of a rectangular specimen.

3. Results and discussion

3.1. Comparison between 0 and 45° specimens

Typical load–deflection curves for the 6.4 mm wide 0 or 45° specimens tested at 77 K and at room temperature are shown in Figs 1a to d separately for each composite before irradiation. For the glass–epoxy (Fig. 1a) and glass–polyimide composites (Fig. 1b), the curves are almost linear up to the failure point for the 0° specimens, whereas for the 45° specimens the curves display a strong nonlinearity for both test temperatures. This is also the case for the carbon–epoxy (Fig. 1c) and carbon–polyimide composites (Fig. 1d).

When a rectangular specimen is loaded at three points, not only flexural stress (tensile and compressive stresses) but also interlaminar shear stress exists at the same time in the specimen [6]. According to the

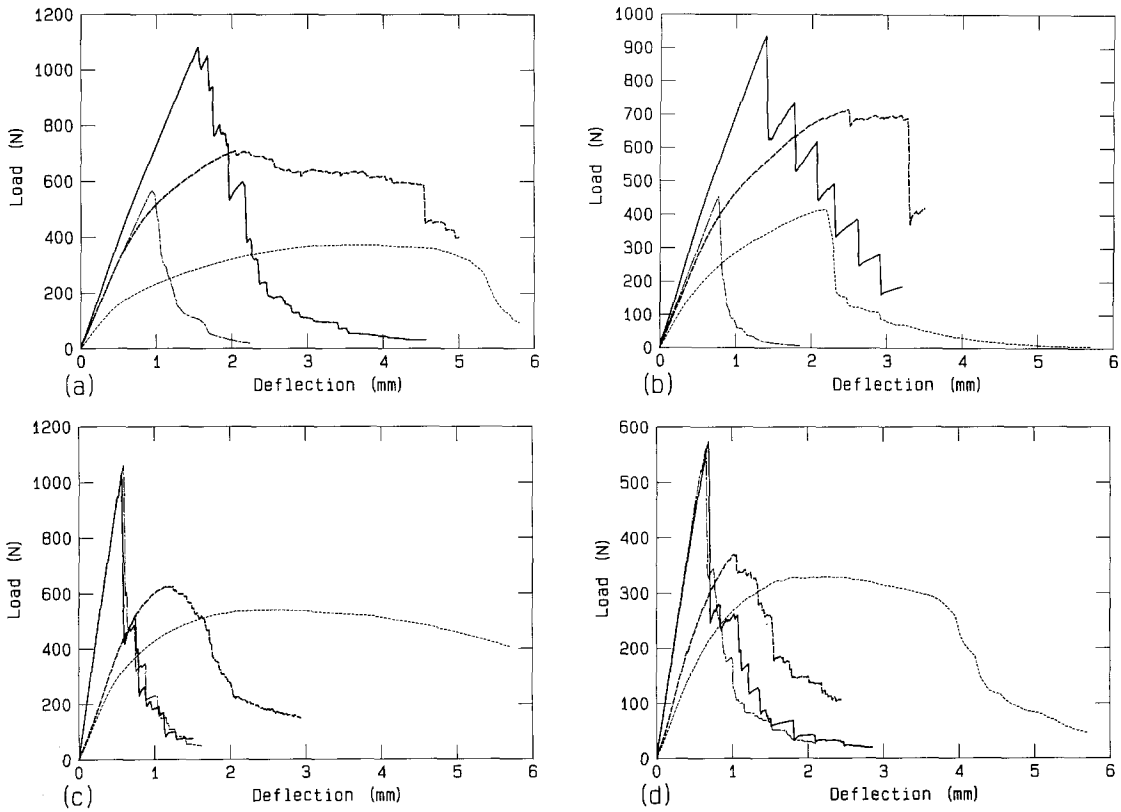

Figure 1 Typical load–deflection curves obtained in three-point bend tests for the 6.4 mm wide 0 or 45° specimens of (a) the glass–epoxy, (b) the glass–polyimide, (c) the carbon–epoxy, and (d) the carbon–polyimide composites before irradiation. The curves are as follows for pairs of the specimen type and the test temperature: (——) 0°/77 K; (– – –) 45°/77 K; (–·–·–·–) 0°/ room temperature; (···) 45°/room temperature.

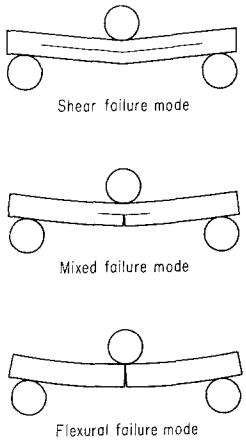

Figure 2 Schematic representation of three types of failure modes observed in three-point bend tests for polymer matrix composites.

Bernoulli-Euler theory [6], the maximum flexural stress, σ_{max}, and the maximum interlaminar shear stress, τ_{max}, exist at the surface of the specimen and at the neutral axis, respectively, and are given by

$$\sigma_{max} = 3P(l/h)/2bh \quad (1)$$

$$\tau_{max} = 3P/4bh \quad (2)$$

where P is the applied load, l is the span length, b is the specimen width, and h is the specimen depth (thickness). From a simplistic standpoint, the specimen can fail in a flexural mode at the surface or in a shear mode at the neutral axis, depending on which of σ_{max} and τ_{max} becomes critical at the failure [6–8]. In practice, however, a mixed failure mode can also occur when the flexural and shear failures take place simultaneously.

A schematic representation of such failure modes has been reported by Hanna and Steingiser [7], and is shown in Fig. 2 in this paper. According to their experimental finding, the failure mode can be determined not only from microscopic or visual examinations of the failed specimen but also from a load–deflection curve of the three-point bend test. When a flexural failure occurs, the specimen fails abruptly without an appreciable decrease in the slope of the load–deflection curve. When a shear failure occurs, on the other hand, the slope of the curve decreases gradually with increasing deflection, and approaches a zero value before the specimen fails completely.

According to this criterion, the 0° specimens tested at 77 K and at room temperature always fail in a flexural mode for all the composites studied here, as seen from the load–deflection curves in Fig. 1. The 45° specimens tested at room temperature, on the other hand, fail in a shear mode for all the composites except the glass–polyimide composite. For this exceptional case, the failure appears to occur in a mixed mode. For the 45° specimens tested at 77 K, the failure appears to occur in a mixed mode for all the composites.

The failure mode thus determined from a load–deflection curve was checked by visual examinations of the failed specimen. The actually observed failure mode was not so simple as depicted schematically in Fig. 2. The characteristics of the respective failure modes shown in Fig. 2, however, were clearly noticed in the failed specimens. For example, no fibre breakage was found for the 45° specimens having a load–deflection curve characteristic of a shear failure mode. For the 0° specimens having a curve characteristic of a flexural failure mode, on the other hand, extensive fibre breakage was observed across the width of the failed specimens.

3.2. Comparison between glass and carbon fibre composites

Typical stress–strain curves for the 6.4 or 12.0 mm wide specimens tested at 77 K and at room temperature are shown in Figs 3a to d separately for each composite before irradiation. In these figures, the interlaminar shear stress calculated from Equation 2 is plotted as a function of the interlaminar shear strain at the specimen neutral axis. This way of plotting is based on the fact that the 45° specimens of the composites studied here always fail in a shear or mixed mode. The interlaminar shear strain, γ, was calculated from [6]

$$\gamma = 2.5\Delta/l \quad (3)$$

where Δ is the midspan deflection.

The stress–strain curves for the glass–epoxy (Fig. 3a) and glass–polyimide composites (Fig. 3b) possess a knee or a change in slope during loading for both specimen widths and for both test temperatures. Comparison of the 6.4 and 12.0 mm wide specimens at each test temperature reveals that the curves are practically identical in the region up to the knee point. The curves appear to be linear in this region, thus suggesting that the 45° specimens of these glass fibre composites are elastic up to the knee point. In the region above the knee point, however, the curves are separated from each other, and consequently the failure point depends on the specimen width.

For the carbon–epoxy (Fig. 3c) and carbon–polyimide composites (Fig. 3d), the stress–strain curves appear to possess no distinct knee point for both specimen widths and for both test temperatures. Comparison of the 6.4 and 12.0 mm wide specimens at each test temperature reveals that the curves are separated from each other from the beginning of loading, thus confirming the absence of a knee point. This fact suggests that the 45° specimens of these carbon fibre composites are inelastic from the very beginning of loading.

Such a difference in the mechanical behaviour between the glass and carbon fibre composites may be due to differences in the mode of load transfer at the fibre–matrix interface and, consequently, in the interfacial bond strength. The fibre–matrix interface is known to have at least two modes of load transfer, i.e. the chemical bond mode and the friction force (mechanical bond) mode [9, 10]. In this connection, Manocha reported that the fibre–matrix bond strength is due for the most part to the friction force mode for carbon fibre-reinforced epoxy composites [11]. This will also be the case for the carbon fibre composites studied here, because the carbon fibres are treated only with an epoxy sizing agent, and hence the chemical bond mode can not be expected to make a significant contribution to the total bond strength at

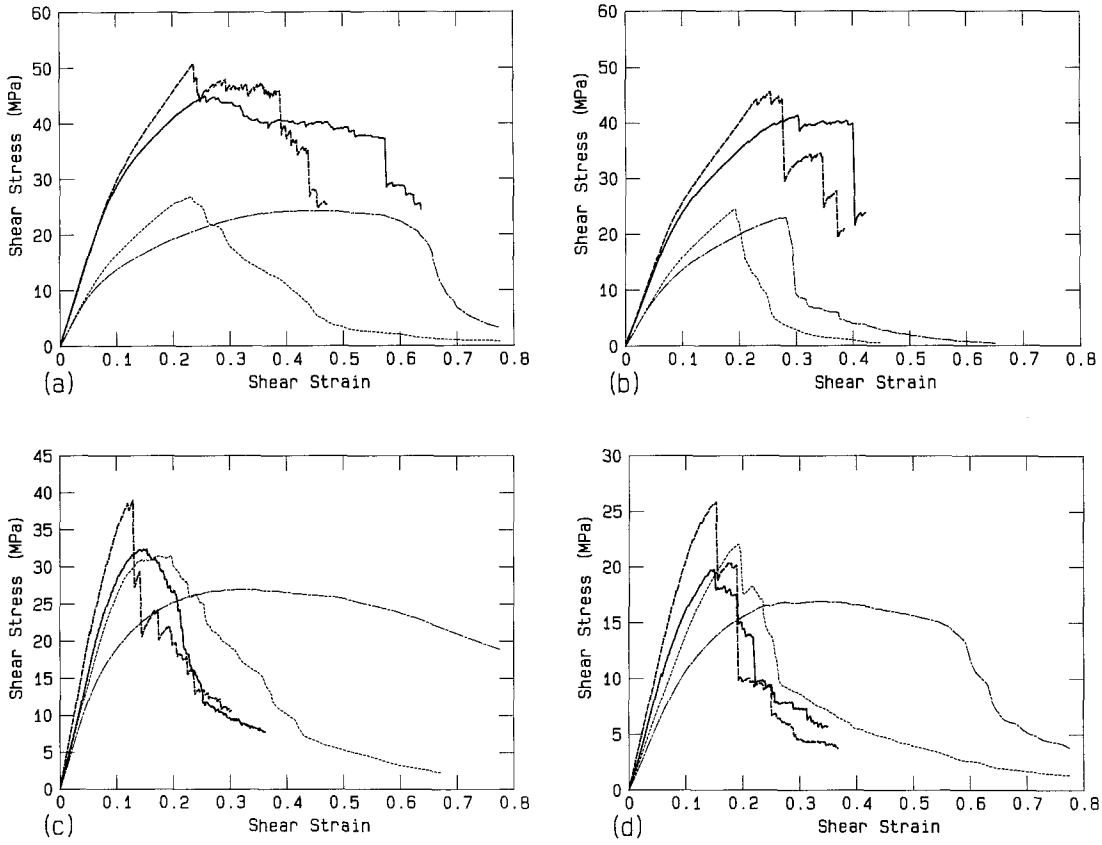

Figure 3 Typical shear stress–strain curves obtained in three-point bend tests for the 6.4 or 12.0 mm wide 45° specimens of (a) the glass–epoxy, (b) the glass–polyimide, (c) the carbon–epoxy, and (d) the carbon–polyimide composites before irradiation. The curves are as follows for pairs of the specimen width and the test temperature: (——) 6.4 mm/77 K; (– – –) 12.0 mm/77 K; (–·–·–·–) 6.4 mm/room temperature; (· · · ·) 12.0 mm/room temperature.

the fibre–matrix interface. For the glass fibre composites, on the other hand, the glass fibres are treated with a silane coupling agent with the intention of increasing the contribution of the chemical bond mode. Then it may be possible that the chemical bond mode is responsible for a knee in the stress–strain curve, because the knee is observed only for the glass–epoxy and glass–polyimide composites (Figs 3a and b).

3.3. Effect of test specimen width

The mechanical properties of the composites before irradiation are summarized in Tables I and II for the 0 and 45° specimens, respectively. In Table I, the Young's (tensile) modulus and the ultimate flexural strength are shown because the 0° specimens of the composites studied here always fail in a flexural mode. The Young's modulus, E, was calculated from [6]

$$E = (P/\Delta)l^3/4bh^3 \quad (4)$$

The initial slope (P/Δ) measurement for this purpose was made at the span length of 60 mm. The ultimate flexural strength was calculated from Equation 1 with $P = P_f$, where P_f is the applied load at failure. The failure test for this purpose was carried out at the span length of 20 mm.

Table I shows that the Young's modulus is almost independent of the specimen width for both test temperatures and for all the composites. The ultimate flexural strength, however, decreases by 1–8% with an increase in the specimen width from 6.4 to 12.0 mm for both test temperatures and for all the composites. This result may be associated with the scatter of the bundle strength of glass or carbon fibres in a composite. Such a scatter will cause the probability of the test specimen failing at a given stress level to increase with an increase in the specimen width, thus leading to a 1–8% decrease in the composite flexural strength.

TABLE I Mechanical properties of 0° specimens before irradiation

Composite	Specimen width (mm)	Young's modulus (GPa)		Ultimate flexural strength (MPa)	
		77 K	RT	77 K	RT
Glass–epoxy	6.4	41.1	34.4	1517	838
	12.0	40.9	34.3	1417	812
Glass–polyimide	6.4	29.1	25.1	1069	521
	12.0	30.2	25.8	1011	516
Carbon–epoxy	6.4	57.6	58.3	884	910
	12.0	56.5	57.5	821	835
Carbon–polyimide	6.4	59.8	60.3	890	855
	12.0	59.5	58.8	845	809

In Table II, the interlaminar shear modulus and the ultimate interlaminar shear strength are shown because the 45° specimens of the composites studied here always fail in a shear or mixed mode. The interlaminar shear modulus, G, was calculated from [6]

$$G = 0.3(P/\Delta)l/bh \quad (5)$$

The ultimate interlaminar shear strength was calculated from Equation 2 with $P = P_f$. The initial slope (P/Δ) and the applied load at failure (P_f) were determined from the failure test made at the span length of 20 mm. For the carbon–epoxy and carbon–polyimide composites, the shear modulus was not evaluated because of the absence of a linear elastic portion in the stress–strain curve.

Table II shows that the shear modulus of the glass–epoxy or glass–polyimide composite is almost independent of the specimen width for both test temperatures. The ultimate shear strength, however, increases by 10–30% with an increase in the specimen width from 6.4 to 12.0 mm for both test temperatures and for all the composites, except the glass–polyimide composite at room temperature.

Comparison of the stress–strain curve between the 6.4 and 12.0 mm wide specimens at each test temperature for each composite (Figs 3a to d) shows that as the specimen width increases, the composite failure mode is shifted from a shear mode to a mixed mode. This fact indicates that the increase in the specimen width results in an increase in the fraction of flexural failure relative to shear failure, thus leading to an enhancement in the reinforcing effect of fibres. Accordingly, the 10–30% increase in the composite shear strength resulting from the specimen width increase from 6.4 to 12.0 mm (Table II) is most likely ascribed to the increased fraction of flexural failure relative to shear failure.

It is interesting to note here that Nardone and Strife [12] reported a similar specimen width dependence of the composite strength for the tensile test of angle-ply graphite–aluminium composites. They also reported that the composite failure mode shifts from a shear mode to a mixed mode with an increase in the specimen width. Such a shift in the composite failure mode appears to be associated with a complexity of the shear stress distribution in the test specimen. For a specimen loaded at three points, for example, Sattar and Kellogg [13] reported a theoretical finding that the interlaminar shear stress is not uniform across the width of the specimen, and that the degree of the nonuniformity increases with an increase in the specimen width. In addition, they reported that the intralaminar (in-plain) shear stress exists in the actual test specimen, although this stress is neglected in the Bernoulli-Euler theory [6]. Then it is quite possible that the nonuniformity of the interlaminar shear stress and the existence of the intralaminar shear stress are responsible for the failure mode shift from a shear mode to a mixed mode. At present, however, further quantitative explanation can not be offered.

3.4. Effect of test temperature

Comparison of the 77 K and room-temperature Young's moduli for 0° specimens (Table I) shows that the modulus is about 18% higher at 77 K than at room temperature for the glass–epoxy and glass–polyimide composites, while for the carbon–epoxy and carbon–polyimide composites the modulus is almost the same between the two temperatures. Such a comparison of the interlaminar shear moduli for 45° specimens (Table II), on the other hand, shows that the modulus is 50–90% higher at 77 K than at room temperature for the glass–epoxy and glass–polyimide composites. These results indicate that the shear modulus of a 45° specimen is much more temperature dependent than the Young's modulus of a 0° specimen.

In general, the Young's modulus of a composite can be represented by the rule of mixtures [14]

$$E_c = E_f V_f + E_m V_m \quad (6)$$

where E is the Young's modulus, V is the volume fraction, and the subscripts c, f, and m stand for the composite, fibre, and matrix, respectively. This equation shows that the composite Young's modulus is dominated primarily by the highest value of the fibre and matrix Young's moduli. The interlaminar shear modulus of a composite, on the other hand, may be approximated by the inverse rule of mixtures [15]

$$1/G_c = V_f/G_p + V_m/G_m \quad (7)$$

where G is the shear modulus. This equation shows that the composite shear modulus is dominated primarily by the lowest value of the fibre and matrix shear moduli. Then it is quite possible that a change in the matrix stiffness with temperature is reflected much more strongly in the composite shear modulus than in the composite Young's modulus, if such a change is small for the fibre stiffness. This will be the case for the

TABLE II Mechanical properties of 45° specimens before irradiation

Composite	Specimen width (mm)	Interlaminar shear modulus (MPa)		Ultimate interlaminar shear strength (MPa)	
		77 K	RT	77 K	RT
Glass–epoxy	6.4	298	157	45.5	22.5
	12.0	298	170	49.5	27.1
Glass–polyimide	6.4	251	165	43.3	24.3
	12.0	249	162	46.2	23.6
Carbon–epoxy	6.4	–	–	33.3	26.8
	12.0	–	–	39.8	31.2
Carbon–polyimide	6.4	–	–	22.2	19.9
	12.0	–	–	28.7	25.0

composites studied here, because the stiffness of the matrix resins used here increases by a factor of about 2 on cooling from room temperature to 77 K [1], thus leading to a 50–90% increase in the composite shear modulus and a mere 18% increase or no appreciable change in the composite Young's modulus (Tables I and II).

Comparison of the 77 K and room temperature ultimate flexural strengths for 0° specimens (Table I) shows that the strength is about 2 times higher at 77 K than at room temperature for the glass–epoxy and glass–polyimide composites, whereas for the carbon–epoxy and carbon–polyimide composites no striking difference in the strength is found between the two temperatures. Such a comparison of the ultimate interlaminar shear strengths for 45° specimens (Table II), on the other hand, shows that the strength is about 2 times higher at 77 K than at room temperature for the glass fibre composites, whereas for the carbon fibre composites the strength is 12–28% higher at 77 K than at room temperature. These results indicate that roughly speaking, the temperature dependence of the shear strength of a 45° specimen is similar to that of the flexural strength of a 0° specimen for all the composites studied here.

An approximate two-fold increase in the flexural strength on cooling to 77 K is attributable mainly to an increase in the bundle strength of E-glass fibres in the glass–epoxy and glass–polyimide composites [1]. A similar increase in the shear strength on cooling to 77 K, on the other hand, appears to be ascribed to factors other than the bundle strength of E-glass fibres. This is because regardless of the test temperature, the 45°specimens fail in a shear or mixed mode, while the 0° specimens fail in a flexural mode, as seen from the load–deflection curves in Fig. 1.

It is generally believed that the composite interlaminar shear strength is dominated primarily by the properties of the matrix and the fibre–matrix interface rather than the fibre [9]. In this connection, it is worth noting that although the ultimate strengths of the matrix resins used in the present work do not change strikingly on cooling from room temperature to 77 K, the Young's moduli of these resins increase by a factor of about 2 [1]. This fact suggests that if the bond strength at the fibre–matrix interface is high enough to transfer full load from the matrix to the fibre, then the temperature dependence of the composite shear strength is virtually determined by the stiffness of the matrix resin. This suggestion will be true for the glass–epoxy and glass-polyimide composites rather than for the carbon-epoxy and carbon–polyimide composites. This is because the fibre–matrix bond strength can be expected to be much higher for the glass fibre composites due to the total contribution of the chemical bond mode and the friction force mode. So far as the glass fibre composites are concerned, therefore, an approximate two-fold increase in the shear strength on cooling to 77 K (Table II) is most likely ascribed to an increase in the matrix stiffness.

For the carbon fibre composites, merely a 12–28% increase in the shear strength on cooling to 77 K (Table II) suggests that the fibre–matrix bond strength is relatively poor for lack of the contribution of the chemical bond mode. Then, the slight increase in the composite shear strength may be associated with the generation of internal shear stresses on cooling to 77 K rather than with an increase in the matrix stiffness. Such stresses will be generated at the fibre–matrix interface by a difference in the thermal expansion between the fibre and the matrix [16]. Possibly the internal shear stresses increase the contribution of the friction force mode to the total bond strength at the interface, thus leading to a 12–28% increase in the composite shear strength on cooling to 77 K.

3.5. Dose dependence of shear modulus

The dose dependence of the interlaminar shear modulus of a 45° specimen was studied by using 6.4 mm wide specimens. The modulus is plotted as a function of absorbed dose in Fig. 4 for the glass–epoxy and glass–polyimide composites. Each data point indicates the average value of three tests, and the error bar shows the standard deviation. A missing error bar means that the deviation is too small to be shown. The shear moduli of these composites are seen to decrease gradually with increasing dose in both the 77 K and room temperature tests. In addition, the dose dependence appears to follow the identical pattern for the two composites at each test temperature.

The degradation of the composite shear modulus appears to be associated with the radiation damage at the fibre–matrix interface rather than in the matrix. This is because a previous work of this series shows that the stiffness of the fibre and matrix materials used here remains practically unchanged even after irradiation up to 170 MGy [1]. In addition, the underlying principle of Equation 7 is that the composite shear modulus is actually determined by the weakest part in the composite. If therefore the fibre–matrix interface is the most radiation sensitive part in the composite, then the composite shear modulus will degrade even if the fibre and matrix stiffness remains unchanged. Thus, the identical dose dependence of the shear modulus for the glass–epoxy and glass–polyimide composites (Fig. 4) reflects a similarity of the fibre–matrix interface between the two composites. The

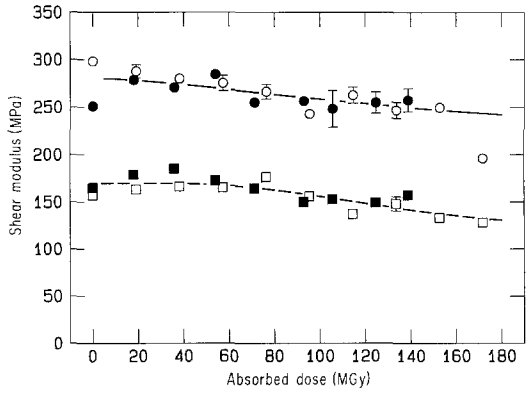

Figure 4 Plot of the interlaminar shear modulus against the absorbed dose in matrix for the 6.4 mm wide 45° specimens of the glass fibre composites. The data points are as follows for pairs of the 77 K and room-temperature tests: (○) glass–epoxy, 77 K; (□) glass–epoxy, RT;(●) glass–polyimide, 77 K; (■) glass–polyimide, RT.

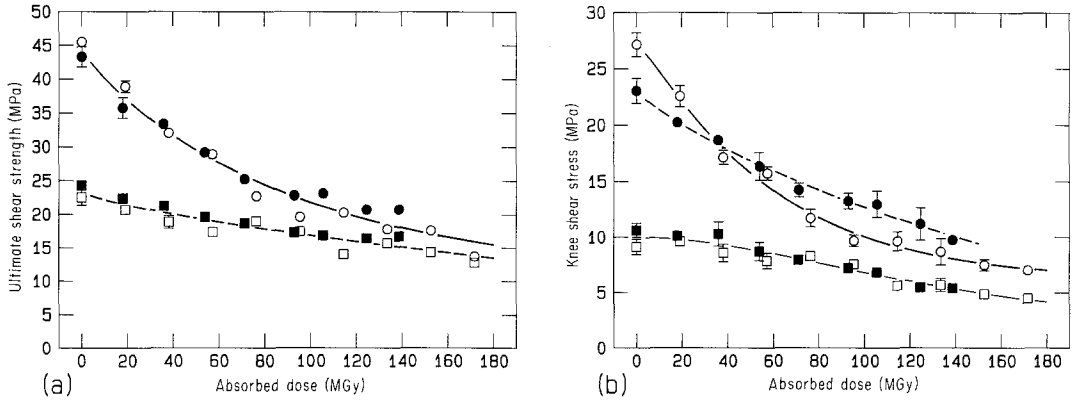

Figure 5 Plots of (a) the ultimate interlaminar shear strength and (b) the interlaminar shear stress at a knee point against the absorbed dose in matrix for the 6.4 mm wide 45° specimens of the glass fibre composites. The data points are as follows for pairs of the 77 K and room-temperature tests: (○) glass–epoxy, 77 K; (□) glass–epoxy, RT; (●) glass–polyimide, 77 K; (■) glass–polyimide, RT.

surface treatment of the glass fibres is, in fact, the same for both of these composites.

3.6. Dose dependence of ultimate shear strength

The dose dependence of the ultimate interlaminar shear strength of a 45° specimen was studied by using 6.4 mm wide specimens. The strength is plotted as a function of absorbed dose in Figs 5 and 6 for the glass and carbon fibre composites, respectively. Figure 5 includes also the interlaminar shear stress at a knee point. The knee shear stress was calculated from Equation 2 with $P = P_k$, where P_k is the applied load at a knee point. In order to determine the knee point, the initial slope in the stress–strain curve was first evaluated from the linear portion of the curve. Then, the position of a knee was determined from a point at which the ratio of stress to strain is 95% of the initial slope. Each data point in Figs 5 and 6 indicates the average value of three tests, and the error bar means the standard deviation.

The plots for the ultimate shear strengths of the glass–epoxy and glass–polyimide composites in Fig. 5a demonstrate that the strengths of these composites decrease monotonically with increasing dose in both the 77 K and room temperature tests. Comparison of the 77 K and room temperature data points shows that a decrease in the strength by irradiation is appreciably greater at 77 K than at room temperature. It is particularly worth noting that the dose dependence at each test temperature follows the identical pattern for the glass–epoxy and glass–polyimide composites. These characteristics of the dose dependence are observed also for the knee shear stress shown in Fig. 5b, except that the knee shear stress at 77 K decreases more rapidly with increasing dose for the glass–epoxy composite than for the glass–polyimide composite. This discrepancy between the two composites is most likely ascribed to a difference in the radiation resistance of the epoxy and polyimide resins (see Figs 8 and 10 in [1]).

The plots for the ultimate shear strengths of the carbon–epoxy and carbon–polyimide composites in Fig. 6 demonstrate that the strengths of these composites decrease monotonically with increasing dose in the 77 K test, whereas in the room temperature test the strengths remain practically unchanged even after irradiation up to 140 MGy. The plots also show that the dose dependence at 77 K follows a rather similar pattern for the carbon–epoxy and carbon–polyimide composites, although the initial strengths of these composites differ significantly from each other. This difference in the initial strength may result from a difference in the volume fraction of fibres for the carbon–epoxy (57%) and carbon–polyimide composites (62%). An example of the interlaminar shear strength decreasing with increasing volume fraction of fibres is, in fact, reported for an S-glass fibre-reinforced epoxy composite [9].

3.7. Degradation mechanism of composite shear strength

In general, the radiation induced degradation of a polymer matrix composite could be due to radiation damage produced in the matrix, at the fibre–matrix interface, and in the fibre. Usually, such damage in the fibre can be neglected, because the radiation resistance of inorganic materials like glass and carbon fibres is much higher than that of organic materials like epoxy and polyimide resins [17]. Then the degradation mechanism of the composite shear strength should be interpreted in terms of radiation damage in the matrix, at the fibre–matrix interface, or both. In this connection,

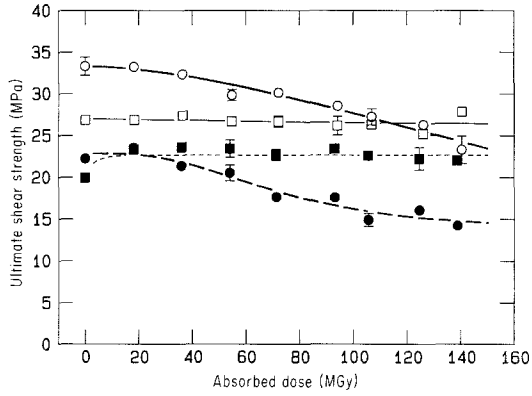

Figure 6 Plot of the ultimate interlaminar shear strength against the absorbed dose in matrix for the 6.4 mm wide 45° specimens of the carbon fibre composites. The data points are as follows for pairs of the 77 K and room-temperature tests: (○) carbon–epoxy, 77 K; (□) carbon–epoxy, RT; (●) carbon–polyimide, 77 K; (■) carbon–polyimide, RT.

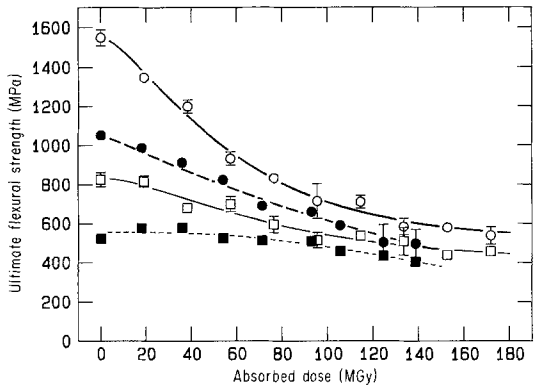

Figure 7 Plot of the ultimate flexural strength against the absorbed dose in matrix for the 6.4 mm wide 0° specimens of the glass fibre composites. The data points are as follows for pairs of the 77 K and room-temperature tests: (○) glass–epoxy, 77 K; (□) glass–epoxy, RT; (●) glass–polyimide, 77 K; (■) glass–polyimide, RT.

a previous work of this series demonstrated that the dose dependence of the ultimate flexural strength of a 0° specimen is virtually determined by a change in the matrix ultimate strain due to irradiation [1]. This degradation mechanism for the flexural strength of a 0° specimen, however, will fail for the ultimate interlaminar shear strength of a 45° specimen, because the 0° and 45° specimens differ essentially from each other in the failure mode (see Fig. 1).

The dose dependence of the ultimate flexural strength is reproduced from a previous paper [1] in Fig. 7 for the glass–epoxy and glass–polyimide composites. The two composites are seen to differ strikingly from each other in the dose dependence of the flexural strength at each test temperature, thus reflecting a difference in the radiation resistance of the epoxy and polyimide resins. However, the two composites are quite similar to each other in the dose dependence of the ultimate shear strength at each test temperature (Fig. 5a). These findings strongly suggest that the degradation of the composite shear strength is associated with the radiation damage at the fibre–matrix interface rather than in the matrix. This idea is consistent with the scanning electron microscope observation reported by Takeda *et al.* [18] for the same glass–epoxy composite as used in the present work. According to their observation made after interlaminar shear tests, the fracture surface of the irradiated composite displays separation or debonding between the fibre and the matrix, thus reflecting the radiation induced decomposition of surface treating compounds at the fibre–matrix interface. It is reasonably concluded, therefore, that the dose dependence of the composite shear strength is virtually determined by a change in the fibre–matrix bond strength due to irradiation.

This degradation mechanism will hold also for the carbon–epoxy and carbon–polyimide composites. Then the dose independent shear strengths of these composites at room temperature (Fig. 6) indicate that the fibre–matrix bond strength is scarcely changed by irradiation up to 140 MGy. In agreement with this view, the scanning electron micrographs reported by Takeda *et al.* [18] for the carbon–epoxy composite show no observable change in the fracture surface even after irradiation up to 120 MGy. The radiation insensitiveness of the fibre–matrix bond strength is perhaps intrinsic of the friction force mode which makes a major contribution to the total bond strength in carbon fibre composites [11].

It should be noted that the friction force mode can function only when the matrix resin is ductile enough to support the fibres at a given strain level. When the matrix resin is brittle, the friction force mode may fail to function properly, and consequently the composite shear strength may come to depend on the matrix brittleness rather than on the fibre–matrix bond strength. In this connection, a previous work of this series shows that the ultimate strains of the epoxy and polyimide resins decrease appreciably on cooling from room temperature to 77 K, and decrease further with increasing absorbed dose (see Fig. 10 in [1]). So far as the carbon fibre composites tested at 77 K are concerned, therefore, the dose dependence of the ultimate shear strength (Fig. 6) is most likely attributed to a change in the matrix brittleness due to irradiation.

4. Conclusions

The present work has shown that the glass–epoxy and glass–polyimide composites are quite similar to each other in the dose dependence of the ultimate interlaminar shear strength of a 45° specimen in both the 77 K and room temperature tests. Comparison of this dose dependence with that for the ultimate flexural strength of a 0° specimen strongly suggests that the dose dependence of the composite shear strength is virtually determined by a change in the fibre–matrix interfacial bond strength due to irradiation.

For the carbon–epoxy and carbon–polyimide composites, the shear strength tested at room temperature changes little even after irradiation up to 140 MGy, while the shear strength tested at 77 K decreases monotonically with increasing absorbed dose. The dose independent shear strength at room temperature is interpreted by assuming that the fibre–matrix bond strength due to the friction force mode is much less sensitive to radiation compared with that due to the chemical bond mode. The dose dependence of the shear strength at 77 K, on the other hand, is attributed to a change in the matrix brittleness due to irradiation, with the recognition that the friction force mode can function only when the matrix resin is ductile to a certain extent.

Acknowledgements

The author is grateful to Mr T. Kanazawa of Japan Atomic Energy Research Institute (JAERI) for his assistance with electron irradiation. Thanks are also due to Dr T. Seguchi of JAERI for kindly reading the manuscript.

References

1. S. EGUSA, *J. Mater. Sci.* **23** (1988) 2753.
2. B. S. BROWN, *J. Nucl. Mater.* **97** (1981) 1.
3. F. W. CLINARD Jr and G. F. HURLEY, *ibid.* **103 & 104** (1981) 705.
4. R. E. FORNES, J. D. MEMORY and N. NARANONG, *J. Appl. Polym. Sci.* **26** (1981) 2061.

5. S. M. MILKOVICH, C. T. HERAKOVICH and G. F. SYKES, *J. Composite Mater.* **20** (1986) 579.
6. C. ZWEBEN, W. S. SMITH and M. W. WARDLE, in "Composite Materials: Testing and Design", ASTM STP 674, edited by S. W. Tsai (American Society for Testing and Materials, 1979) p. 228.
7. G. L. HANNA and S. STEINGISER, in "Composite Materials: Testing and Design", ASTM STP 460 (American Society for Testing and Materials, 1969) p.182.
8. A. W. CHRISTIANSEN, J. LILLEY and J. B. SHORTALL, *Fibre Sci. Technol.* **7** (1974) 1.
9. L. J. BROUTMAN, in "Modern Composite Materials", edited by L. J. Broutman and R. H. Krock (Addison-Wesley, Massachusetts, 1967) Ch. 13.
10. C. C. CHAMIS, in "Composite Materials", Vol. 6, edited by E. P. Plueddemann (Academic Press, New York, 1974) Ch. 2.
11. L. M. MANOCHA, *J. Mater Sci.* **17** (1982) 3039.
12. V. C. NARDONE and J. R. STRIFE, *ibid.* **22** (1987) 592.
13. S. A. SATTAR and D. H. KELLOGG, in "Composite Materials: Testing and Design", ASTM STP 460 (American Society for Testing and Materials, 1969) p. 62.
14. R. H. KROCK and L. J. BROUTMAN, in "Modern Composite Materials", edited by L. J. Broutman and R. H. Krock (Addison-Wesley, Massachusetts, 1967) Ch. 1.
15. H. T. CORTEN, *ibid.* Ch. 2.
16. M. B. KASEN, *Cryogenics* **21** (1981) 323.
17. R. D. HAY and E. J. RAPPERPORT, Oak Ridge National Laboratory Report ORNL/TM-2643 (1976).
18. N. TAKEDA, S. KAWANISHI, A. UDAGAWA and M. HAGIWARA, *J. Mater. Sci.* **20** (1985) 3003.

Received 22 February 1988
and accepted 24 July 1989